Domain patterns in copolymer-homopolymer mixtures

Aya Ito*
Meme Media Laboratory, Hokkaido University, Sapporo 060-0812, Japan
(Received 18 May 1998)

We introduce a dynamical model and carry out computer simulations for phase separation of diblock copolymer-homopolymer mixtures. The homopolymer chains are assumed to be compatible with one of the blocks of the diblock copolymers whereas the two blocks of the diblock copolymer chains are mutually incompatible. In this system, two kinds of phase separation, namely macrophase separation of diblock copolymers and homopolymers and microphase separation in diblock copolymers, take place simultaneously by decreasing temperature. Depending on the strength of the interactions, the domain pattern and its ordering process are changed. We can see both phenomena. One is macrophase separation, which dominates the time evolution of the system; the other is the formation of the mesoscale structure in the whole of the system. We show some typical phase-separated patterns and investigate the kinetics of phase ordering of these patterns by evaluating structure factors. [S1063-651X(98)02711-1]

PACS number(s): 83.70.Hq, 64.75.+g

I. INTRODUCTION

We study domain growth in diblock copolymer-homopolymer mixtures during the phase-separation process. It is well known that there are two representatives of phase-separation phenomena. One is macrophase separation of binary mixtures and the other is microphase separation in block copolymers.

In a mixture of two different homopolymers which are mutually incompatible, a phase separation takes place at low temperatures. The homopolymers segregate each other and the system forms a domain structure. These domains grow in time and the time dependence of their averaged domain size l obeys $l \sim t^{1/3}$. Thus we can observe the phase separation in polymer blends in a macroscopic length scale, which is called macrophase separation [1].

On the other hand, a block copolymer system gives a prototype in which microphase separation occurs. When each block is incompatible with each other, the block copolymer system also experiences a phase separation just after quenching. However, because of the connectivity of blocks, they cannot separate in a macroscopic length scale. As a consequence, they form a spatially periodic structure in equilibrium with a period comparable to polymer size [3–9].

Now, how does the system which consists of a block copolymer and a homopolymer experience the phase-separation phenomena at low temperature [2]? As far as the spatial structures in equilibrium are concerned, there are some theoretical and experimental studies in copolymer-homopolymer mixtures [10–14]. In particular, the morphology in equilibrium has been investigated experimentally in A-B block copolymer–A homopolymer mixtures (A-B/A system) where one block chain of a block copolymer and homopolymer chain consist of the same monomer segments, and hence various domain patterns are observed [11–13].

According to the experimental results in A-B/A systems, the ratio of the polymerization indices of a block copolymer to homopolymer is a key parameter for domain growth and morphology. Let N_A, N_B, and N_{homo} be the polymerization indices of A block, B block, and homopolymer. Roughly speaking, experimentalists observed that when $N_{\mathrm{homo}} \gg N_A$, the copolymer-homopolymer mixture undergoes macrophase separation of copolymers and homopolymers and then in copolymer-rich domains, microphase separation starts during the evaporation process of solvent. On the other hand, in the case of $N_{\mathrm{homo}} \lesssim N_A$, the system does not experience a phase separation in a macroscopic length scale and the mesoscale structure is formed in the whole of the system in equilibrium. However, the dynamics of phase separation in block copolymer-homopolymer mixtures has not been studied enough either theoretically or experimentally.

We have investigated the dynamics and morphology in phase separation in diblock copolymer-homopolymer mixtures. The aim of our study is to introduce a dynamical model of A-B/C systems and to understand the kinetics and the relation between the kinetics and morphology in block copolymer and homopolymer mixtures [2].

In the previous paper, we have investigated the dynamics of phase separation in A-B/C systems in which macrophase separation of copolymers and homopolymers occurs at first and as the phase separation proceeds, microphase separation starts in the copolymer-rich domain. Our results explain the formation of a curious pattern called ''onion-ring,'' which is obtained in real experiments in A-B/A systems with the $N_{\mathrm{homo}} \gg N_A$ condition.

In this paper we study the pattern formation in copolymer-homopolymer mixtures wherein both phenomena are obtained. One is macrophase separation, which dominates the time evolution of the system. The other is the formation of the mesoscale structure in the whole of the system in equilibrium.

The organization of this paper is as follows. In Sec. II, we introduce a simple dynamical model in terms of the local volume fractions of each monomer. In Sec. III, we carry out computer simulations in two dimensions, using the cell dynamical method [15]. Computer simulations show that two kinds of phase separations take place simultaneously. The

*Present address: Institute for Global Change Research, Frontier Research System for Global Change, SEAVANS North 7F, 1-2-1 Shibaura, Minato-ku, Tokyo 105-6791, Japan.

phase-separated pattern is varied by changing the interaction parameters, which arise from the monomer-monomer interaction and the configurational entropy of polymer chains. In Sec. IV, we calculate the structure factors in order to investigate the kinetics of the above phase separations. In Sec. V we give a discussion.

II. THE MODEL EQUATIONS

We consider the system which consists of A-B diblock copolymers and C homopolymers. The polymerization indices of these polymers are N_A, N_B, and N_C, respectively. The block ratio of a block copolymer f is defined by $f=N_A/(N_A+N_B)$. The local volume fractions of these monomers are denoted by ϕ_A, ϕ_B, and ϕ_C. In this paper, we restrict ourselves to diblock copolymers with $f=\frac{1}{2}$ (or $N_A=N_B$), in order to understand the essence of the phase-separation phenomena of A-B/C systems.

Under the incompressibility condition, two of the local volume fractions are independent. It is convenient to take $\psi=\phi_A+\phi_B$ and $\phi=\phi_A-\phi_B$ as the independent variables. The variable ψ is useful to describe the segregation of copolymers and homopolymers while ϕ plays the role of an order parameter in a microphase separation. Furthermore, we use $\eta=\psi-\psi_c$ instead of ψ, where ψ_c is the volume fraction at the critical point of the phase separation of copolymers and homopolymers.

The model free energy for copolymer-homopolymer mixtures in terms of η and ϕ consists of short-range and long-range parts,

$$F\{\eta,\phi\}=F_S\{\eta,\phi\}+F_L\{\eta,\phi\}. \tag{1}$$

The short-range part is written as follows:

$$F_S\{\eta,\phi\}=\frac{D_1}{2}\int d\mathbf{r}(\nabla\eta(\mathbf{r}))^2+\frac{D_2}{2}\int d\mathbf{r}(\nabla\phi(\mathbf{r}))^2 + \int d\mathbf{r}\{f_\eta(\eta)+f_\phi(\phi)+f_{\rm int}(\eta,\phi)\}. \tag{2}$$

The functions f_η and f_ϕ are assumed to be an even function and to have double minima below the respective critical temperature. We choose the following interactions between η and ϕ:

$$f_{\rm int}(\eta,\phi)=b_1\eta\phi-\frac{b_2}{2}\eta\phi^2+\frac{b_4}{2}\eta^2\phi^2. \tag{3}$$

Here we omit $-b_3\eta^2\phi/2$ because $b_3=b_0(1/N_A-1/N_B)$ with b_0 a positive constant, which vanishes for $N_A=N_B$. For the same reason, we also omit terms which are proportional to $\eta\phi^3$ and $\eta^3\phi$. The first term in $f_{\rm int}$, $b_1\eta\phi$ arises from the monomer-monomer interactions. The energy from these interactions is written as

$$\tfrac{1}{2}\sum_{i,j}u_{i,j}\int d\mathbf{r}\,\phi_i\phi_j, \tag{4}$$

where $i,j=A,B,C$ and $u_{i,j}$ stands for the interaction strength between i and j monomers. The interaction strength b_1 is given by $u_{i,j}$ as follows:

$$b_1=\tfrac{1}{4}(u_{AA}-u_{BB})-\tfrac{1}{2}(u_{AC}-u_{BC}). \tag{5}$$

If the repulsive interaction strength u_{BC} between B and C is large enough, b_1 is positive.

The second and the last terms in $f_{\rm int}$ arise from the configurational entropy of polymer chains. The second term $-b_2\eta\phi^2/2$ represents the fact that microphase separation should occur only in the copolymer-rich phase. The last term $b_4\eta^2\phi^2/2$ brings out the fact that two kinds of phase separation—phase separation of copolymers and homopolymers and microphase separation in block copolymers—control each other. The coefficients b_2 and b_4 depend on polymerization indices. The ratio is given by $b_2/b_4=\sqrt{N_C}/(\sqrt{N_{AB}}+\sqrt{N_C})$ with $1/N_{AB}=(1/N_A+1/N_B)/2$. Its range is $0<b_2/b_4<1$. If $N_{AB}\gg N_C$, then $b_2/b_4\to 0$, and $b_2/b_4\to 1$ for $N_C\gg N_{AB}$.

In the experiments of phase separation in A-B/A systems, the ratio of polymerization indices of a copolymer to a homopolymer is one of the key parameters. We can take the effect of the ratio of polymerization indices on phase separation in A-B/C systems by changing b_2/b_4.

In this system, there is a long-range interaction term F_L whose origin is the connectivity of A and B blocks in a diblock copolymer,

$$F_L\{\phi\}=\frac{\alpha}{2}\int\int d\mathbf{r}\,d\mathbf{r}'G(\mathbf{r},\mathbf{r}')[\phi(\mathbf{r})-\overline{\phi}][\phi(\mathbf{r}')-\overline{\phi}], \tag{6}$$

where $G(\mathbf{r},\mathbf{r}')$ is Green function defined by $-\nabla^2G(\mathbf{r},\mathbf{r}')=\delta(\mathbf{r}-\mathbf{r}')$ and $\overline{\phi}$ is the spatial average of ϕ. The coefficient α is given by $\alpha=\sigma/N^2$ with $N=N_A+N_B$ and a positive constant σ. Here we set $\overline{\phi}=0$ since $N_A=N_B$. In general, $F_L\{\eta,\phi\}$ has the following form in A-B/C systems:

$$F_L\{\eta,\phi\}=\int\int d\mathbf{r}\,d\mathbf{r}'G(\mathbf{r},\mathbf{r}')\left\{\frac{\alpha}{2}[\phi(\mathbf{r})-\overline{\phi}][\phi(\mathbf{r}')-\overline{\phi}]+\beta[\eta(\mathbf{r})-\overline{\eta}][\phi(\mathbf{r}')-\overline{\phi}]+\frac{\gamma}{2}[\eta(\mathbf{r})-\overline{\eta}][\eta(\mathbf{r}')-\overline{\eta}]\right\}, \tag{7}$$

where $\overline{\eta}$ is the spatial average of η. However, we choose $\beta=\gamma=0$, because β and γ are proportional to $(1/N_A-1/N_B)$. As is mentioned already, we are concerned with the $N_A=N_B$ case here.

Using the above free energy F, we write a dynamical model of phase separation in a copolymer-homopolymer mixture as

$$\frac{\partial\eta}{\partial t}=L_1\nabla^2\frac{\delta F\{\eta,\phi\}}{\delta\eta}, \tag{8a}$$

$$\frac{\partial\phi}{\partial t}=L_2\nabla^2\frac{\delta F\{\eta,\phi\}}{\delta\phi}, \tag{8b}$$

where L_1 and L_2 are transport coefficients. The relative mag-

nitude of these coefficients is not known experimentally, so that we set $L_1=L_2=1$ simply.

We have already explained our model except $b_4\eta^2\phi^2/2$ in the previous paper [2]. In this paper we investigate phase separation and its dynamical process of the general A-B/C system bringing the effect of the chain length.

III. COMPUTER SIMULATIONS

A. Cell dynamical method

We carry out computer simulations of the model system in two dimensions, using the cell dynamical method [15]. In two dimensions, the space is divided into 128×128 square cells with periodic boundary conditions. The size of a cell is set to unity.

The cell dynamical system corresponding to the partial differential equation (PDE) (8) is written as follows:

$$\eta(t+\Delta t;i,j)=\eta(t;i,j)+\langle\langle\mathcal{J}_\eta\rangle\rangle-\mathcal{J}_\eta(t;i,j), \tag{9a}$$

$$\phi(t+\Delta t;i,j)=\phi(t;i,j)+\langle\langle\mathcal{J}_\phi\rangle\rangle-\mathcal{J}_\phi(t;i,j) -\alpha[\phi(t;i,j)-\overline{\phi}], \tag{9b}$$

where

$$\mathcal{J}_\eta(t;i,j)=-D_1(\langle\langle\eta\rangle\rangle-\eta)-A_\eta\tanh\,\eta+\eta+b_1\phi -\tfrac{1}{2}b_2\phi^2+b_4\eta\phi^2, \tag{10a}$$

$$\mathcal{J}_\phi(t;i,j)=-D_2(\langle\langle\phi\rangle\rangle-\phi)-A_\phi\tanh\,\phi+\phi+b_1\eta -b_2\eta\phi+b_4\eta^2\phi, \tag{10b}$$

and

$$\langle\langle X\rangle\rangle=\tfrac{1}{6}\sum_{\mathrm{NN}}X+\tfrac{1}{12}\sum_{\mathrm{NNN}}X. \tag{11}$$

In the PDE model written by Eqs. (8) and (1), the order parameters are continuous variables. However, in the cell dynamical systems, the order parameters η and ϕ are defined in each cell. $\eta(t;i,j)$ stands for local order parameter on the (i,j)th cell at time t. We choose f_η and f_ϕ as

$$\frac{df_\eta}{d\eta}=A_\eta\tanh\,\eta-\eta, \tag{12a}$$

$$\frac{df_\phi}{d\phi}=A_\phi\tanh\,\phi-\phi. \tag{12b}$$

Above each critical temperature $A_i<1$ and below $A_i>1$ ($i=\eta,\phi$). The subscripts NN and NNN stand for nearest-neighbor and next-nearest-neighbor cells, respectively.

In the original cell dynamical method by Oono and coworkers, they set $\Delta t=1$, however we choose $\Delta t=0.5$ in order to avoid numerical instability in the case of $D_1=0.8$ and 1.0. This also relieves the anisotropy of the domain in the late stage of domain growth, which arises from the discretization of space. We follow the original method except for this point.

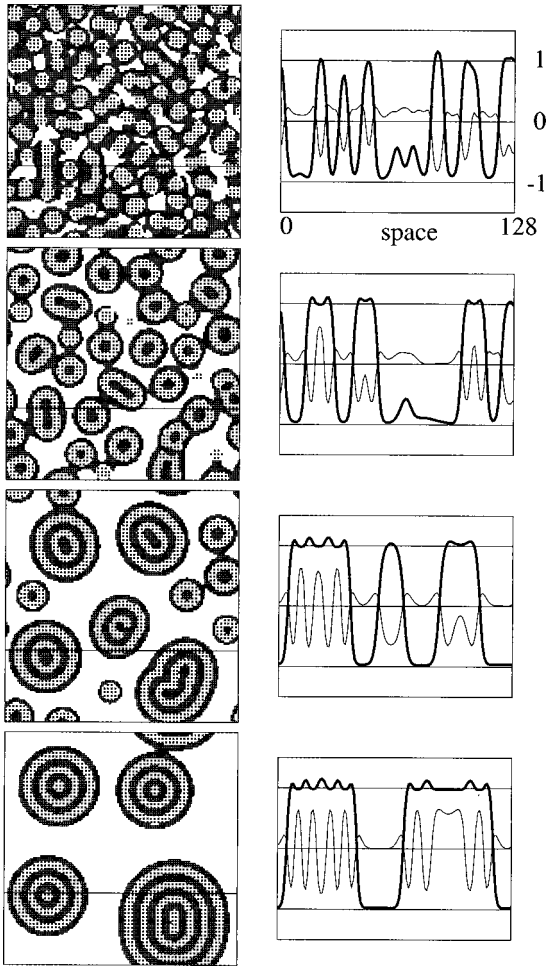

FIG. 1. Domain pattern at $t=2000.0$, 8000.0, 64 000.0, and 1 024 000.0 from the top to the bottom in which parameters are $\overline{\eta}=-0.2$, $\overline{\phi}=0.0$, $D_1=1.0$, $D_2=0.5$, $A_\eta=1.3$, $A_\phi=1.1$, and $\alpha=0.02$. The interaction parameters are $b_1=0.07$, $b_2=0.2$, and $b_4=0.0$. Gray and black colors in the domain pattern indicate the regions in which $\eta>0.0$ and $\phi>0.15$, respectively. The bold line represents the profile of η and the thin line is that of ϕ along the line $y=40$.

B. Domain pattern for $b_2\neq0$ and $b_4=0$

First, we show the domain growth in the presence of the term $-b_2\eta\phi^2/2$ arising from the configurational entropy. As is mentioned that $b_2/b_4=\sqrt{N_C}/(\sqrt{N_{AB}}+\sqrt{N_C})$, when $N_A=N_B$, if $N_C\gg N_A$, then $b_2/b_4\approx1$. In this case we can omit the higher-order term $b_4\eta^2\phi^2/2$.

We start from initial random conditions. The ranges of η and ϕ at $t=0.0$ are $\overline{\eta}-s<\eta<\overline{\eta}+s$ and $\overline{\phi}-s<\phi<\overline{\phi}+s$, with $s=0.01$. (These initial conditions will also be used hereafter.)

Figure 1 displays the domain growth where the parameters are $\overline{\eta}=-0.2$, $\overline{\phi}=0.0$, $D_1=1.0$, $D_2=0.5$, $\alpha=0.02$, $A_\eta=1.3$, and $A_\phi=1.1$. The interaction parameters are $b_1=0.07$, $b_2=0.2$, and $b_4=0$. The left figures in Fig. 1 show the domain patterns at $t=2000.0$, 8000.0, 64 000.0, and 1 024 000.0 from the top to the bottom. The regions in which $\eta>0$ are drawn by a gray color. Thus, the gray color regions stand for copolymer-rich domains, while white color regions represent homopolymer-rich domains. Microphase separa-

tion of a block copolymer can take place in copolymer-rich domains and/or the area near the interface between copolymer-rich and homopolymer-rich domains. The regions where $\phi > 0.15$ are shown by a black color. These are A block rich domains which appear as the result of microphase separation of block copolymers. We represent the phase separation pattern of homopolymer-copolymer mixtures by superimposing a black color pattern on a gray color one. The right-side figures in Fig. 1 show the order-parameter profile along the line $y = 40$. The bold line is the profile of η, the thin line represents that of ϕ.

At an early stage, $t = 2000.0$, phase separation of copolymers and homopolymers takes place at first. A blocks aggregate near the interface between copolymers and homopolymers because of the interaction $b_1 \eta \phi$. After $t = 8000.0$, macrophase separation of copolymers and homopolymers proceeds. Then in the copolymer-rich domain microphase separation of diblock copolymers takes place because of the interaction $-b_2 \eta \phi^2/2$.

In this case we have chosen a suitable value of b_1 for the repulsive interaction between the B block and a homopolymer, so that the A block rich domain is formed at the interface between block copolymers and homopolymers and that the target pattern called ''onion-ring'' appears [2]. We can see the animation of domain growth with an increasing number of rings [16]. For small values of b_1, the microphase separated pattern does not form rings. This morphological transition is discussed in our previous paper. Furthermore, when we choose b_1 too large, macrophase separation is prevented.

C. Domain pattern for $b_2 \neq 0$ and $b_4 \neq 0$

Next we show the domain pattern where both $-b_2 \eta \phi^2/2$ and $b_4 \eta^2 \phi^2/2$ interaction terms are present in A-B/C systems. Figure 2 shows the phase-ordering process for the parameters $\bar{\eta} = 0.0$, $\bar{\phi} = 0.0$, $D_1 = 1.0$, $D_2 = 0.5$, $\alpha = 0.002$, $A_\eta = 1.29$, and $A_\phi = 1.27$. The interaction parameters are $b_1 = 0.11$, $b_2 = 0.2$, and $b_4 = 0.4$. We choose b_2 and b_4 as $b_2/b_4 = 0.5$. This choice comes from the $N_A = N_C$ condition. The left figures in Fig. 2 show the domain patterns at $t = 2000.0$, 8000.0, 32 000.0, and 1 024 000.0 from the top to the bottom. The gray and black areas in the domain pattern show $\eta > \bar{\eta} = 0.0$ and $\phi > 0.3$, respectively. The right-side figures in Fig. 2 show the order parameter profiles along the line $y = 64$. We change the definitions of the black and gray areas depending on the figures in order to understand well the characteristics of the phase-ordering process.

At an early stage, $t = 2000.0$, both macrophase separation and microphase separation take place. We can see that because of the $b_1 \eta \phi$ term, the phases of η and ϕ tend to be opposite to each other from their profiles. Thus the homopolymer-rich domain (white color area) formed by macrophase separation is almost covered with the A block rich domain (black color area) which appears as the result of microphase separation of block copolymers. The segregation of homopolymers and the A block of block copolymers is not clear yet. In the late stage of phase ordering, after $t = 8000.0$, η begins to form a lamellar pattern, and A block rich regions are formed at the interface between $\eta > 0$ and $\eta < 0$. The white color homopolymer rich domains appear

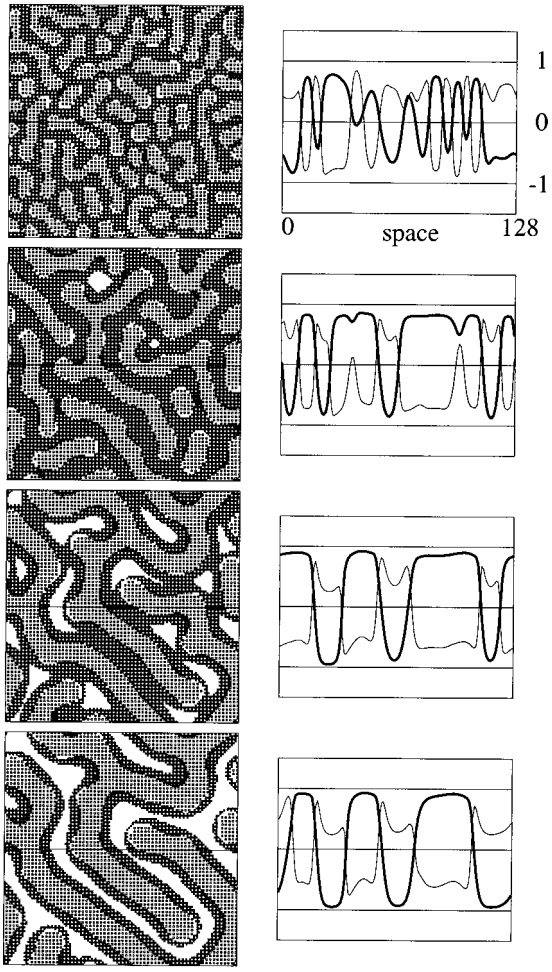

FIG. 2. Domain pattern at $t = 2000.0$, 8000.0, 32 000.0, and 1 024 000.0 from the top to the bottom in which parameters are $\bar{\eta} = \bar{\phi} = 0.0$, $D_1 = 1.0$, $D_2 = 0.5$, $A_\eta = 1.29$, $A_\phi = 1.27$, and $\alpha = 0.002$. The interaction parameters are $b_1 = 0.11$, $b_2 = 0.2$, and $b_4 = 0.4$. Gray and black colors in the domain pattern indicate the regions in which $\eta > \bar{\eta} = 0.0$ and $\phi > 0.3$, respectively. The bold line represents the profile of η and the thin line is that of ϕ along the line $y = 64$.

gradually. After $t = 32\,000.0$, phase separation of copolymers and homopolymers does not develop, and the winding domain pattern becomes the straight lamellar one. Therefore, we obtain the ''bilayer'' pattern in which the A-B block copolymer behaves like an amphiphilic molecular [17]. Thus in the copolymer domain, the A block faces homopolymers, while the B block rich region forms inside. In this case, macrophase separation does not take place. And the ordering domain with some finite size is formed by phase separation of copolymers and homopolymers.

In Fig. 3 we display the domain pattern and its profile for a smaller value of b_1, $b_1 = 0.05$. Other parameters are the same as those in Fig. 2. In this case, macrophase separation of copolymers and homopolymers is dominant. At an early stage, $t = 2000$, both phase separations take place similarly to the case in Fig. 2. After $t = 8000.0$, we can see that at the interface between $\eta > 0$ and $\eta < 0$, a black area appears to be torn, and that macrophase separation develops. The repulsive

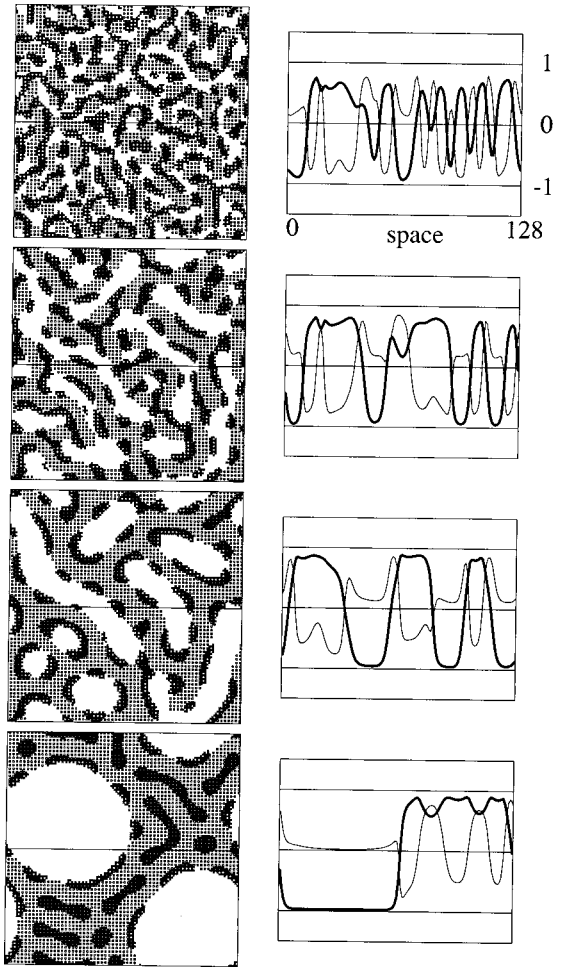

FIG. 3. Domain pattern at $t=2000.0$, 8000.0, 32000.0 and 1 024000.0 from the top to the bottom for $b_1=0.05$. Other parameters are the same as those in Fig. 2.

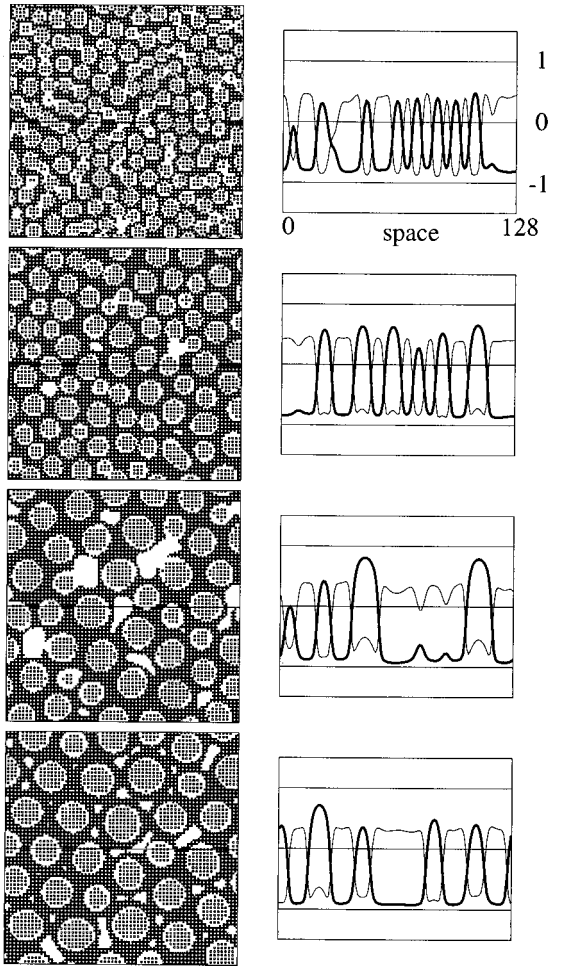

FIG. 4. Domain pattern at $t=2000.0$, 8000.0, 64 000.0, and 1 024 000.0 from the top to the bottom in which parameters are $\overline{\eta}=-0.5$, $\overline{\phi}=0.0$, $D_1=0.8$, $D_2=0.5$, $A_\eta=A_\phi=1.27$, and $\alpha=0.002$. The interaction parameters are $b_1=0.1$, $b_2=0.0$, and $b_4=0.4$. Gray and black colors in the domain pattern indicate the regions in which $\eta>\overline{\eta}=-0.5$ and $\phi>0.3$, respectively. The bold line represents the profile of η and the thin line is that of ϕ along the line $y=64$.

interaction between the *B* block and homopolymers is not sufficient to control macrophase separation. In this process of macrophase separation, the homopolymer-rich domain shown by a white color forms a spherical domain although $\overline{\eta}=0$. We set f_η as an even function of η as described already. However, the effective potential of η is not an even function because of the interaction terms. Thus, we can see in the domain pattern and its profile in Fig. 3 that $\eta\simeq-1$ in the white color area, while the local average of η is smaller than 1 in the copolymer-rich area. The spatial average of η in the whole of the system has to be $\overline{\eta}=0$, so that the white color area should be less than half of the system. This is the reason why the white domains constitute a spherical shape.

For $A_\eta=1.29$ and $A_\phi=1.27$ as in Figs. 2 and 3, both macrophase separation and microphase separation take place. However, in the case of Fig. 3, because of the interaction $-b_2\eta\phi^2/2$ and $b_4\eta^2\phi^2/2$ terms which arise from configurational entropy, macrophase separation controls microphase separation at the $\eta>\frac{1}{2}$ and $\eta<0$ regions. $[(-b_1\eta+b_4\eta^2)\phi^2/2$ is positive when $\eta>\frac{1}{2}$ and $\eta<0.]$ Furthermore, in the case of Fig. 2, b_1 is large, so that the *A* block aggregates strongly at the interface between copolymer- and homopolymer-rich regions and that this *A* block domain suppresses macrophase separation.

D. Domain pattern for $b_2=0$ and $b_4\neq0$

We present the phase-ordering processes for $b_2=0$. This can be considered as the $N_A\gg N_C$ limit. Although $b_2\eta\phi^2/2$ is lower order than $b_4\eta^2\phi^2/2$ in the expansion in terms of η and ϕ, we consider the case $b_2=0$ as the limiting case.

In Fig. 4 we display the pattern formation for the parameters $\overline{\eta}=-0.5$, $\overline{\phi}=0.0$, $D_1=0.8$, $D_2=0.5$, $\alpha=0.002$, and $A_\eta=A_\phi=1.27$. The interaction parameters are $b_1=0.1$, $b_2=0.0$, and $b_4=0.4$. The domain patterns and the profiles at $t=2000.0$, 8000.0, 64 000.0, and 1 024 000.0 are shown. The gray and the black color areas stand for $\eta>\overline{\eta}=-0.5$ and $\phi>0.3$, respectively.

At the early stage $t=2000.0$, both macrophase and microphase separation take place. We can see that because of the $b_1\eta\phi$ term, the phases of η and ϕ tend to be opposite to each other from their profiles. Until $t=64\,000.0$, domain growth proceeds and the gray color droplet becomes bigger in time. However, after $t=64\,000.0$, domain growth is suppressed, and the system begins to make a favorable structure; the size of the domains seems to be monodisperse and the

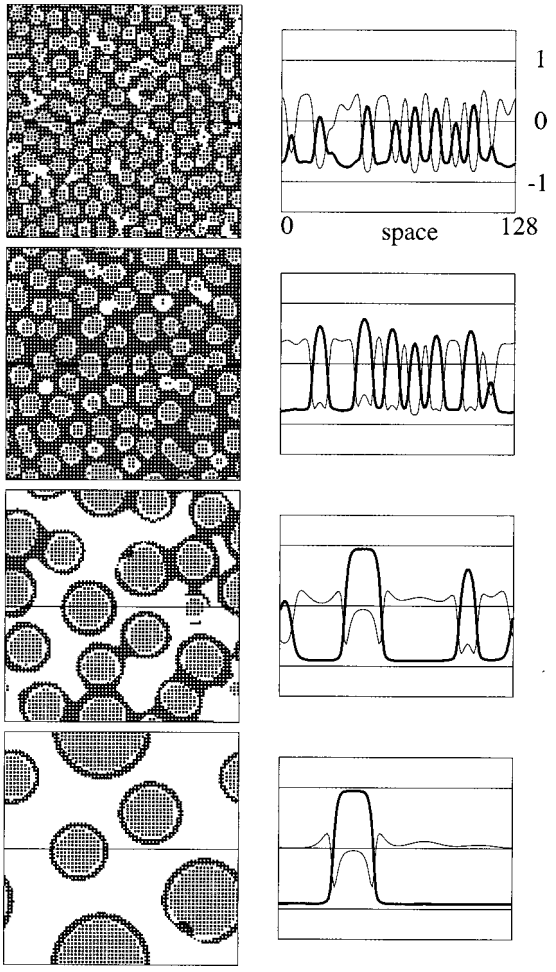

FIG. 5. Domain pattern at $t=2000.0$, 8000.0, 64 000.0, and 1 024 000.0 from the top to the bottom for $b_1=0.05$. Other parameters are the same as those in Fig. 4. Gray and black colors in the domain pattern indicate the regions in which $\eta>\overline{\eta}=-0.5$ and $\phi>0.2$, respectively.

gray color domain looks like it is being placed on a triangular lattice. The A block rich region shown by a black color is formed at the interface between $\eta>\overline{\eta}$ and $\eta<\overline{\eta}$. We note that this domain pattern is similar to the ''micelle'' pattern observed in A-B/A experiments with the $N_A \gg N_{\mathrm{homo}}$ condition.

We note from the profile at $t=1\,024\,000.0$ that the spatial variation of ϕ is small in the homopolymer-rich area ($\eta<0$), compared with that in Fig. 2; the height of the profile of ϕ in the black color A block rich domain is less than that in Fig. 2. This smallness of ϕ at the interface comes from the shape of the gray color spherical domain.

In Fig. 5, we show the domain pattern and its profile for smaller value of b_1, $b_1=0.05$. In this case the system undergoes macrophase separation of diblock copolymers and homopolymers. At the early stage $t=2000.0$, we can see that two kinds of phase separation take place. However, at the later stage, after $t=64\,000.0$, microphase separation is suppressed on account of the $b_4\eta^2\phi^2/2$ term. Because of the smallness of b_1, the $b_1\eta\phi$ term cannot control macrophase separation. It causes barely nonuniformity of ϕ near the interface of the macrophase separated domain.

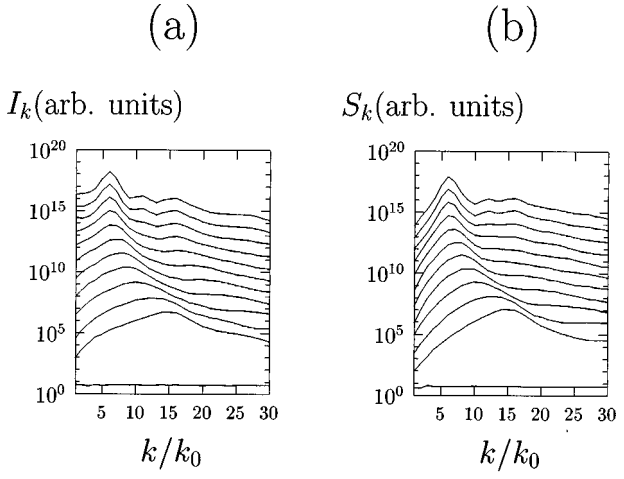

FIG. 6. Spherical averaged structure factors (a) I_k and (b) S_k are depicted as a function of the wave number, in a semilogarithmic plot at $t=1000.0$, 2000.0, 4000.0, 8000.0, 16 000.0, 32 000.0, 64 000.0, 128 000.0, 256 000.0, 514 000.0, and 1 024 000.0 from the bottom to the top. The parameters are the same as those in Fig. 4. The unit of the wave number is given by $k_0=\pi/64$.

IV. SCATTERING FUNCTIONS

In order to analyze the kinetics of the domain growth, we calculate the time evolution of scattering functions, $I_{\mathbf{k}}$ and $S_{\mathbf{k}}$ at each time step, where $I_{\mathbf{k}}(t)=\langle \eta_{\mathbf{k}}\eta_{-\mathbf{k}}\rangle$ and $S_{\mathbf{k}}(t)=\langle \phi_{\mathbf{k}}\phi_{-\mathbf{k}}\rangle$. Here, $\eta_{\mathbf{k}}$ and $\phi_{\mathbf{k}}$ are the Fourier component of $\eta(\mathbf{r})$ and $\phi(\mathbf{r})$, respectively. The average $\langle\ \rangle$ is taken over the initial randomness. The scattering intensities are averaged over 10 independent runs.

In Fig. 6, we show the time evolution of the spherical averaged structure factor I_k and S_k for the parameters which are the same as those in Fig. 4. We plot the relative intensity (a) I_k and (b) S_k versus wave number in a semilogarithmic plot, at $t=1000.0$, 2000.0, 4000.0, 8000.0, 16 000.0, 32 000.0, 64 000.0, 128 000.0, 256 000.0, 5 120 000.0, and 1 024 000.0 from the bottom to the top. Each curve is arbitrarily shifted along the intensity axis to distinguish among the curves. We pay attention to the maximum peak position of I_k and S_k as the characteristic wave number of the system. The maximum peak position k_M of I_k in Fig. 6(a) becomes smaller and smaller in time until $t=64\,000.0$. After $t=64\,000.0$, k_M does not change. In the same manner, in Fig. 6(b), the peak position k_M of S_k becomes smaller and smaller in time until $t=128\,000.0$. After that k_M does not change. As is shown in Fig. 4, phase separation does not develop after $t=64\,000.0$. The time evolution of k_M of I_k and S_k reflects it.

In order to investigate domain growth, we summarize in Figs. 7, 8, and 9 the time evolution of the peak position of the spherical average of the structure factor in a double logarithmic plot.

Figure 7 displays k_M of I_k and S_k versus time for the same parameters as those in Fig. 1. The characteristic wave number obtained from I_k and S_k is shown with $\diamond$ and $+$, respectively. The solid line indicates the slope $-\frac{1}{3}$. From k_M of I_k, it is obvious that domain growth by phase separation of diblock copolymers and homopolymers follows $k_M \sim t^{-1/3}$, as in ordinary binary mixtures. On the other hand, we can see

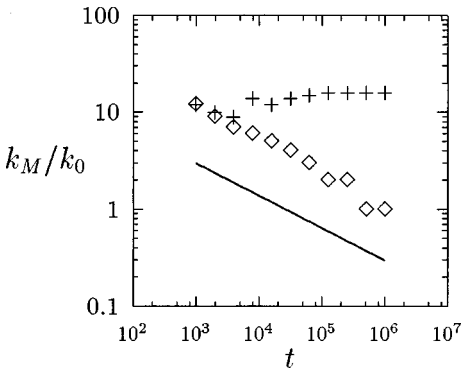

FIG. 7. Time evolution of the peak position. The parameters are $\bar{\eta}=-0.2$, $\bar{\phi}=0.0$, $D_1=1.0$, $D_2=0.5$, $A_\eta=1.3$, $A_\phi=1.1$, $\alpha=0.02$, $b_1=0.07$, $b_2=0.2$, and $b_4=0.0$. These parameters are the same as those in Fig. 1. The unit of the wave number is given by $k_0=\pi/64$.

from k_M of S_k that at early times the characteristic wave number of ϕ is very close to that of η, because the spatial variation of $\phi(\mathbf{r})$ is caused by $\eta(\mathbf{r})$ through the interaction $b_1\eta\phi$ as was mentioned in the preceding section. Furthermore, after $t=8000.0$, k_M of S_k abandons to follow that of I_k and shows the characteristic wave number of microphase separated domains because microphase separation begins to take place in diblock copolymer-rich domains.

Figures 8(a) and 8(b) display k_M of I_k and S_k versus time for the parameters corresponding to those in Figs. 2 and 3, respectively, in the same manner as Fig. 7. In Fig. 8(a), the characteristic wave number of η decreases smoothly with $k_M\sim t^{-1/3}$ in the early stage of phase separation. However, k_M of I_k does not change after $t=16\,000.0$. The characteristic wave number k_M of S_k also decreases at first and does not change in the later stage. In this case, microphase separation occurs from the beginning because of $A_\phi=1.27$, which is large enough to cause microphase separation. This microphase separation progresses with the strong correlation with η because of a large value of b_1. Thus the characteristic wavelength of ϕ is so close to that of η, and at $t=32\,000.0$, k_M of S_k catches up to that of I_k. After that, the characteristic wave number of ϕ also does not change.

In contrast to this, the system undergoes macrophase separation in Fig. 8(b). Up to $t=32\,000.0$ microphase separation takes place with phase separation of copolymers and homopolymers. However, macrophase separation does not stop in this case. After $t=32\,000.0$, k_M of S_k shows the domain size of microphase separation in a diblock copolymer-rich domain. It is noted that the final value of k_M of S_k in (a) is not identical with but smaller than that in (b).

In Figs. 9(a) and 9(b), we show the time evolution of the characteristic wave number k_M of I_k and S_k, in which the parameters are the same as those in Figs. 4 and 5, respectively. These are plotted in the same manner as in Figs. 7 and 8. In Fig. 9(a), the time evolution of k_M of I_k and S_k is shown and is similar to that in Fig. 8(a). The characteristic wave number of η decreases at an early stage of phase separation and then ceases to change after $t=64\,000.0$. And k_M of S_k almost follows that of I_k.

In Fig. 9(b), both k_M of I_k and S_k decrease in time during a phase-separation process. In this system, macrophase separation of copolymers and homopolymers takes place, and the characteristic wave number of η decreases with $k_M\sim t^{-1/3}$. Nonuniformity of ϕ is caused only at the interface between the homopolymer and the copolymer, thus k_M of S_k decreases following that of I_k.

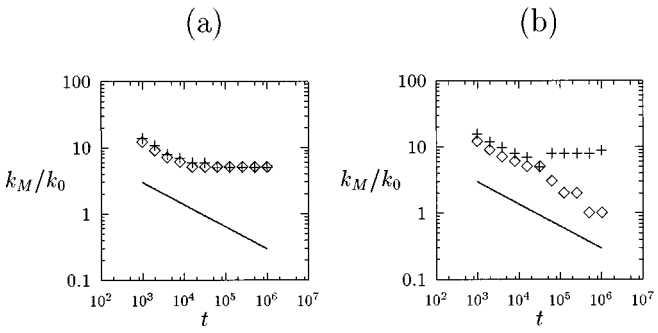

FIG. 8. Time evolution of the peak position for (a) $b_1=0.11$ and (b) $b_1=0.05$. Other parameters are the same as those in Figs. 2 and 3.

V. DISCUSSION

We have studied the phase separation in copolymer-homopolymer mixtures. Computer simulations of the model equations have realized that two kinds of phase separation take place simultaneously. One of the features of our simulation is that we can observe both phenomena of macrophase separation and the formation of mesoscale structure in the whole system. In the former case, the *A*-*B* block copolymer separates from the homopolymer, as one component of the polymer blends. However, in the latter case, the strong repulsive interaction between *B* and *C* lets the *A*-*B* block copolymer work as an amphiphilic molecular. We have obtained bilayer and micelle patterns as the typical patterns of the latter case.

In Figs. 2 and 3 or 4 and 5, for small values of b_1 macrophase separation takes place, while for large values of b_1 a mesoscale structure is formed. We can see that whether macrophase separation occurs or not is determined by the competition between $b_1\eta\phi$ and $-b_2\eta\phi^2/2+b_4\eta^2\phi^2/2$. This is roughly understood as follows.

In these systems both macrophase separation of copolymers and homopolymers described by η and microphase separation described by ϕ take place because of $A_\eta=1.29$ or

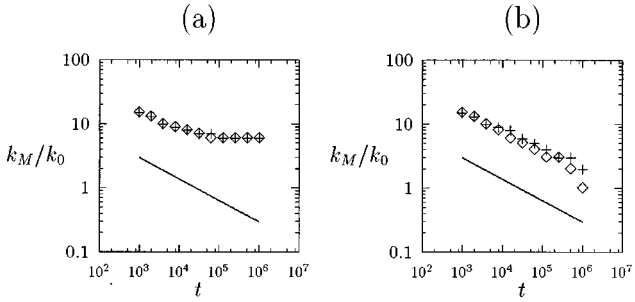

FIG. 9. Time evolution of the peak position for (a) $b_1=0.1$ and (b) $b_1=0.05$. Other parameters are the same as those in Figs. 4 and 5.

1.27 and $A_\phi = 1.27$. Now, the presence of $-b_2\eta\phi^2/2$ and $b_4\eta^2\phi^2/2$ works macrophase separation to control microphase separation. Thus in Figs. 3 and 5, a macrophase separated pattern appears. On the other hand, the $b_1\eta\phi$ term which arises from the repulsive interaction between B and C monomers makes a wall of A block at the interface between the copolymer and the homopolymer. This wall prevents η from diffusing through it, thus macrophase separation is controlled for large b_1. In this way, the mesoscale structures are formed in the case of Figs. 2 and 4.

The essential difference between Figs. 2 and 4 is not only $\overline{\eta}$ but also b_4. If $\overline{\eta}$ is larger in Fig. 2, as in Fig. 4 we scarcely obtain bilayer or sticklike domain.

There is a periodicity of the domain patterns in the mesoscale structure in Figs. 2 and 4. However, it is not so clear how to estimate the characteristic wavelength in our Landau free-energy approach. Thus, the average size of the domain by phase separation of copolymers and homopolymers is not determined. The above point is left as a future problem.

ACKNOWLEDGMENTS

The author wishes to thank Professor T. Ohta for a critical reading of the manuscript and for helpful suggestions. She would like to acknowledge the advice and the hospitality of Professor Y. Nishiura and Professor R. Kobayashi, and other members of the Nonlinear Studies and Computation Group of Research Institute for Electronic Science in Hokkaido University. She expresses her sincere gratitude to Professor Y. Tanaka of Meme Media Laboratory in Hokkaido University. She also would like to express her appreciation to Professor T. Yamagata of Frontier Research System for Global Change.

[1] D. J. Gunton, M. S. Miguel and P. S. Sahni, *Phase Transition and Critical Phenomena* (Academic, New York, 1983), Vol. 8, p. 267.
[2] T. Ohta and A. Ito, Phys. Rev. E **95**, 5250 (1995).
[3] S. A. Brazovskii, Zh. Eksp. Teor. Fiz. **68**, 175 (1975) [Sov. Phys. JETP **41**, 85 (1975)].
[4] L. Leibler, Macromolecules **13**, 1602 (1980).
[5] T. Ohta and K. Kawasaki, Macromolecules **19**, 2621 (1986).
[6] A. N. Semenov, Zh. Eksp. Teor. Fiz. **88**, 1242 (1985) [Sov. Phys. JETP **61**, 733 (1985)].
[7] F. S. Bates and G. H. Fredrickson, Annu. Rev. Phys. Chem. **41**, 525 (1990).
[8] T. Inoue, T. Soen, and T. Hashimoto, J. Polym. Sci., Polym. Phys. Ed. **7**, 1283 (1969).
[9] D. A. Hadjuk *et al.*, Macromolecules **27**, 4063 (1994).
[10] K. M. Hong and J. Noolandi, Macromolecules **16**, 1083 (1983).
[11] H. Tanaka, H. Hasegawa, and T. Hashimoto, Macromolecules **24**, 240 (1991).
[12] S. Koizumi, H. Hasegawa, and T. Hashimoto, Macromolecules **27**, 6532 (1994).
[13] S. Koizumi, H. Hasegawa, and T. Hashimoto, Macromolecules **27**, 7893 (1994).
[14] K. I. Winey, E. L. Thomas, and L. J. Fetters, Macromolecules **25**, 2645 (1992).
[15] Y. Oono and S. Puri, Phys. Rev. Lett. **58**, 836 (1987); S. Puri and Y. Oono, Phys. Rev. A **38**, 1542 (1988); M. Bahiana and Y. Oono, *ibid.* **41**, 6763 (1990).
[16] A. Ito, T. Ohta, and D. Ueyama, *Phase Separation in Polymer Systems*, video animation (Hokkaido University, Sapporo, Japan, 1997).
[17] T. Kawakatsu, Phys. Rev. E **50**, 2856 (1994).